A Study of the Gluon Ladder in Diffractive Processes

Jeppe R. Andersen* [a], Agustín Sabio Vera†‡ [b]

a Cavendish Laboratory, University of Cambridge, Madingley Road, CB3 0HE Cambridge, UK
b II. Institut für Theoretische Physik, Universität Hamburg, Luruper Chaussee 149, 22761 Hamburg, Germany

February 2, 2008

Abstract

The solution to the non–forward BFKL equation in the Leading Logarithmic approximation is expressed in terms of a sum of iterations of its kernel directly in transverse momentum and rapidity space. Several studies of the non–forward solution are performed both at the level of the gluon Green's function and for a toy cross–section, including an analysis of the diffusion properties as found in this approach. The method developed in this paper allows for a direct inspection of the momenta in the BFKL ladder, and can be applied to solving the non–forward BFKL equation to next–to–leading logarithmic accuracy, when the corresponding kernel is available.

*e-mail: andersen@hep.phy.cam.ac.uk
†e-mail: sabio@mail.desy.de
‡Alexander von Humboldt Research Fellow

1 Introduction

An interesting framework to study the behaviour of QCD scattering amplitudes in the limit of large centre–of–mass energies $\sqrt{s}$ and fixed momentum transfer $\sqrt{-t}$ is the Balitsky–Fadin–Kuraev–Lipatov (BFKL) formalism [1]. The BFKL framework can be applied to processes characterised by a colour octet exchange as well as colour singlet exchange (diffractive processes). The case of $t = 0$ colour singlet scattering corresponds to forward scattering, whereas the case of $t \neq 0$ is called non–forward scattering. The optical theorem relates the amplitude for forward diffractive scattering to the amplitude for a colour octet exchange, which will be exploited in the check of some of the results derived in this paper. If the momentum transfer is perturbative, i.e. $-t \gg \Lambda^2_{\rm QCD}$, it is possible to use the non–forward BFKL equation to study high–t diffraction in the high energy limit, which is characterised by a final state with two systems with transverse momentum $-t$ and far apart in rapidity. The colour singlet exchange in the non–forward case results in a rapidity gap in jet activity. The non–forward BFKL equation thus provides a useful theoretical framework to study diffractive physics from first principles in QCD.

The differential cross–section for diffractive scattering,

$$\frac{{\rm d}\sigma}{{\rm d}t} \;=\; \frac{|A(s,t)|^2}{16\pi s^2}, \tag{1}$$

can be described within the BFKL framework by a factorised scattering amplitude of the form

$$\frac{|A(s,t)|}{s} \;=\; \left| \int {\rm d}^2\mathbf{k}_a \int {\rm d}^2\mathbf{k}_b \, \Phi_{\rm A}(\mathbf{k}_a,\mathbf{q}) \, \Phi_{\rm B}(\mathbf{k}_b,\mathbf{q}) \, \frac{f\left(\mathbf{k}_a,\mathbf{k}_b,\mathbf{q},{\rm Y}\right)}{(\mathbf{k}_a-\mathbf{q})^2\mathbf{k}_b^2} \right|, \tag{2}$$

where Y is the rapidity separation of the scattered probes, $\Phi_{\rm A}(\mathbf{k}_a,\mathbf{q})$ and $\Phi_{\rm B}(\mathbf{k}_b,\mathbf{q})$ are the process–dependent impact factors and the four–point gluon Green's function, $f(\mathbf{k}_a,\mathbf{k}_b,\mathbf{q},{\rm Y})$, is universal. For illustration, in Fig. 1 a typical dominant contribution to this colour singlet exchange in the high energy limit is shown. As explained below in Sec. 2 the non–forward BFKL equation describes the evolution of $f(\mathbf{k}_a,\mathbf{k}_b,\mathbf{q},{\rm Y})$ as a function of the rapidity separation Y. This formalism can be applied, for example, to the study of the diffractive production of vector mesons in photon–proton collisions at HERA for large center–of–mass energies and transverse momentum squared $|t| > \Lambda^2_{\rm QCD}$. In this kinematical region the Leading Logarithm (LL) terms $(\alpha_s \ln s/|t|)^n$ generated in the perturbative series must be resummed. Non–perturbative contributions are included in the proton parton densities and in the meson light–cone wave function present in the corresponding impact factor. For the ρ, ϕ and J/ψ mesons the transverse momentum spectrum and spin density matrix elements have recently been measured at HERA [2]. From the theoretical side, there has been an intense activity in the study of these processes, see e.g. Ref. [3]. The case of photon dissociating to a photon has also been studied in Ref. [4]. Another example of the application of this approach is the description of events with interjet rapidity gaps in photon–hadron and hadron–hadron collisions [5].

The original analytic solution to the non–forward LL BFKL equation [6] proved to be significantly more complicated than its forward counterpart. In order to exhibit the conformal invariance that proved vital in solving the forward BFKL equation, it is necessary to perform a Fourier transform from transverse momentum space to impact parameter representation. The non–forward BFKL equation at next–to–leading logarithmic (NLL) accuracy $(\alpha_s \, (\alpha_s \ln s/|t|)^n$

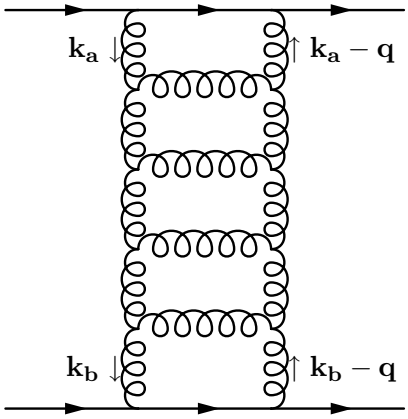

Figure 1: A Feynman diagram contributing to the LL approximation for quark–quark scattering with colour singlet exchange.

terms) will be significantly more complicated, with the conformal invariance being explicitly broken by the running of the coupling (as it happens in the NLL forward case [7]). It is therefore important to investigate new strategies to find the solution to this equation.

In this paper we present a new approach to obtaining the solution to the non–forward BFKL equation to LL accuracy. The method of solution is based on the separation of different contributions to the BFKL kernel by a phase space slice. Once this separation is performed it is possible to apply an iterative approach similar to the one presented in Ref. [8] for the case of the BFKL equation describing a colour octet exchange. This approach has recently been generalised [9] to solve this BFKL equation in the NLL approximation both in QCD and $N=4$ supersymmetric Yang–Mills theory [10] (reviews can be found in [11]).

In the present work we concentrate on extending this iterative approach to the solution of the BFKL equation describing diffractive processes. The presented method of solving the BFKL equation directly in transverse momentum space has the benefit that it allows for a direct inspection of all involved momenta. In particular it is possible to study the diffusion of the transverse scales along the evolution in rapidity. The same method of solution can be applied to the non–forward BFKL equation in the NLL approximation. The corresponding analysis will be performed when the calculation of the non–forward NLL kernel is completed [12].

The structure of this paper is as follows. In section 2 the LL BFKL equation in the non–forward case is presented and the phase space slicing regularisation procedure is performed. In section 3 the non–forward LL BFKL equation is solved by iterating the kernel, obtaining in this way an explicit expression for the four–point gluon Green's function. In section 4 the behaviour of the four–point gluon Green's function is analysed for different values of the momentum transfer. A study of the diffusion properties is performed of not just the four–point gluon Green's function, but also, in section 5, for cross–sections calculated with toy impact factors. The conclusions are presented at the end.

2 The Non–Forward LL BFKL Equation

The LL BFKL equation describing colour singlet exchange with a non–zero momentum transfer squared, $-t = \mathbf{q}^2$, was originally calculated in Ref. [1]. The starting point in the present work will be Eq. (4.16) of Ref. [13] where the integral equation for the Mellin transform in rapidity of the four–point gluon Green's function, $f_\omega(\mathbf{k}_a, \mathbf{k}_b, \mathbf{q})$, is given by

$$\begin{aligned}\omega f_\omega(\mathbf{k}_a,\mathbf{k}_b,\mathbf{q}) &= \delta^{(2)}(\mathbf{k}_a-\mathbf{k}_b)+\frac{\bar{\alpha}_s}{2\pi}\int d^2\mathbf{k}'\left[\frac{-\mathbf{q}^2}{(\mathbf{k}'-\mathbf{q})^2\mathbf{k}_a^2}f_\omega(\mathbf{k}',\mathbf{k}_b,\mathbf{q})\right.\\ &+\frac{1}{(\mathbf{k}'-\mathbf{k}_a)^2}\left(f_\omega(\mathbf{k}',\mathbf{k}_b,\mathbf{q})-\frac{\mathbf{k}_a^2}{\mathbf{k}'^2+(\mathbf{k}_a-\mathbf{k}')^2}f_\omega(\mathbf{k}_a,\mathbf{k}_b,\mathbf{q})\right)\\ &\left.+\frac{1}{(\mathbf{k}'-\mathbf{k}_a)^2}\left(\frac{(\mathbf{k}_a-\mathbf{q})^2\mathbf{k}'^2}{(\mathbf{k}'-\mathbf{q})^2\mathbf{k}_a^2}f_\omega(\mathbf{k}',\mathbf{k}_b,\mathbf{q})-\frac{(\mathbf{k}_a-\mathbf{q})^2}{(\mathbf{k}'-\mathbf{q})^2+(\mathbf{k}_a-\mathbf{k}')^2}f_\omega(\mathbf{k}_a,\mathbf{k}_b,\mathbf{q})\right)\right], \qquad (3)\end{aligned}$$

where $\mathbf{k}_a$ and $\mathbf{k}_b$ describe the two–dimensional transverse momenta of the exchanged gluons in the t–channel (see Fig. 1) and we define $\bar{\alpha}_s \equiv \alpha_s N_c/\pi$. The driving term $\delta^{(2)}(\mathbf{k}_a-\mathbf{k}_b)$ corresponds to a simple two gluon exchange. It is more convenient to rearrange the terms in this expression and, as the integration variable, to use the transverse momenta of the s–channel gluons, $\mathbf{k} = \mathbf{k}' - \mathbf{k}_a$, i.e.

$$\begin{aligned}\omega f_\omega(\mathbf{k}_a,\mathbf{k}_b,\mathbf{q}) &= \delta^{(2)}(\mathbf{k}_a-\mathbf{k}_b)\\ &+\frac{\bar{\alpha}_s}{2\pi}\int d^2\mathbf{k}\left\{\left[\frac{1}{\mathbf{k}^2}\left(1+\frac{(\mathbf{k}_a-\mathbf{q})^2(\mathbf{k}+\mathbf{k}_a)^2}{(\mathbf{k}+\mathbf{k}_a-\mathbf{q})^2\mathbf{k}_a^2}\right)-\frac{\mathbf{q}^2}{(\mathbf{k}+\mathbf{k}_a-\mathbf{q})^2\mathbf{k}_a^2}\right]f_\omega(\mathbf{k}+\mathbf{k}_a,\mathbf{k}_b,\mathbf{q})\right.\\ &\left.-\frac{1}{\mathbf{k}^2}\left(\frac{\mathbf{k}_a^2}{(\mathbf{k}+\mathbf{k}_a)^2+\mathbf{k}^2}+\frac{(\mathbf{k}_a-\mathbf{q})^2}{(\mathbf{k}+\mathbf{k}_a-\mathbf{q})^2+\mathbf{k}^2}\right)f_\omega(\mathbf{k}_a,\mathbf{k}_b,\mathbf{q})\right\}. \qquad (4)\end{aligned}$$

At this stage it is possible to separate the exchange terms form the s–channel contributions by introducing a phase space slicing parameter λ (at NLL it is useful to use dimensional regularisation to show the cancellation of infrared divergences, at LL this is not needed). It is also convenient to use the following approximation

$$\begin{aligned}f_\omega(\mathbf{k}+\mathbf{k}_a,\mathbf{k}_b,\mathbf{q}) &= f_\omega(\mathbf{k}+\mathbf{k}_a,\mathbf{k}_b,\mathbf{q})\left(\theta\left(\mathbf{k}^2-\lambda^2\right)+\theta\left(\lambda^2-\mathbf{k}^2\right)\right)\\ &\simeq f_\omega(\mathbf{k}+\mathbf{k}_a,\mathbf{k}_b,\mathbf{q})\,\theta\left(\mathbf{k}^2-\lambda^2\right)+f_\omega(\mathbf{k}_a,\mathbf{k}_b,\mathbf{q})\,\theta\left(\lambda^2-\mathbf{k}^2\right). \qquad (5)\end{aligned}$$

In all the results presented in this paper we have made sure this approximation is valid by checking that the four–point Green's function is insensitive to the value of the slicing parameter for small values of λ.

Therefore, the non–forward BFKL equation for the Green's function can be written in a very simple form:

$$\begin{aligned}\left(\omega-\omega_0(\mathbf{k}_a,\mathbf{q},\lambda)\right)f_\omega(\mathbf{k}_a,\mathbf{k}_b,\mathbf{q}) &= \delta^{(2)}(\mathbf{k}_a-\mathbf{k}_b)\\ &+\int\frac{d^2\mathbf{k}}{\pi\mathbf{k}^2}\theta\left(\mathbf{k}^2-\lambda^2\right)\xi(\mathbf{k}_a,\mathbf{k},\mathbf{q})\,f_\omega(\mathbf{k}+\mathbf{k}_a,\mathbf{k}_b,\mathbf{q}). \qquad (6)\end{aligned}$$

In order to write the equation in this way the following notation has been introduced:

$$\xi\left(\mathbf{k}_a,\mathbf{k},\mathbf{q}\right) = \frac{\bar{\alpha}_s}{2}\left(1+\frac{\left(\mathbf{k}_a-\mathbf{q}\right)^2\left(\mathbf{k}+\mathbf{k}_a\right)^2-\mathbf{q}^2\mathbf{k}^2}{\left(\mathbf{k}+\mathbf{k}_a-\mathbf{q}\right)^2\mathbf{k}_a^2}\right), \tag{7}$$

and

$$\begin{aligned}\omega_0\left(\mathbf{k}_a,\mathbf{q},\lambda\right) &= \frac{\bar{\alpha}_s}{2\pi}\int\frac{d^2\mathbf{k}}{\mathbf{k}^2}\left[\theta\left(\lambda^2-\mathbf{k}^2\right)\left(1+\frac{\left(\mathbf{k}_a-\mathbf{q}\right)^2\left(\mathbf{k}+\mathbf{k}_a\right)^2-\mathbf{q}^2\mathbf{k}^2}{\left(\mathbf{k}+\mathbf{k}_a-\mathbf{q}\right)^2\mathbf{k}_a^2}\right)\right. \\ &- \left.\frac{\mathbf{k}_a^2}{\left(\mathbf{k}+\mathbf{k}_a\right)^2+\mathbf{k}^2}-\frac{\left(\mathbf{k}_a-\mathbf{q}\right)^2}{\left(\mathbf{k}+\mathbf{k}_a-\mathbf{q}\right)^2+\mathbf{k}^2}\right].\end{aligned} \tag{8}$$

The latter expression corresponds to the Regge trajectory in our regularisation. In the case of $\mathbf{q}=\mathbf{0}$, the trajectory for the colour–octet exchange should be obtained, and indeed we find

$$\omega_0\left(\mathbf{k}_a,\mathbf{0},\lambda\right) = \frac{\bar{\alpha}_s}{\pi}\int\frac{d^2\mathbf{k}}{\mathbf{k}^2}\left[\theta\left(\lambda^2-\mathbf{k}^2\right)-\frac{\mathbf{k}_a^2}{\left(\mathbf{k}+\mathbf{k}_a\right)^2+\mathbf{k}^2}\right] = -\bar{\alpha}_s\ln\frac{\mathbf{k}_a^2}{\lambda^2}. \tag{9}$$

Moreover, the whole solution to the non–forward BFKL equation has the correct limit for $q\to 0$ as found in Ref. [8].

The expression for the non–forward LL Regge trajectory can be simplified if we make use of the forward limit in Eq. (9), i.e.

$$\begin{aligned}\omega_0\left(\mathbf{k}_a,\mathbf{q},\lambda\right) &= \frac{1}{2}\left(\omega_0\left(\mathbf{k}_a,\mathbf{0},\lambda\right)+\omega_0\left(\mathbf{k}_a-\mathbf{q},\mathbf{0},\lambda\right)\right) \\ &+ \frac{\bar{\alpha}_s}{2\pi}\int\frac{d^2\mathbf{k}}{\mathbf{k}^2}\,\theta\left(\lambda^2-\mathbf{k}^2\right)\left(\frac{\left(\mathbf{k}_a-\mathbf{q}\right)^2\left(\mathbf{k}+\mathbf{k}_a\right)^2-\mathbf{q}^2\mathbf{k}^2}{\left(\mathbf{k}+\mathbf{k}_a-\mathbf{q}\right)^2\mathbf{k}_a^2}-1\right).\end{aligned} \tag{10}$$

The last integral is negligible when λ is small, and therefore the non–forward trajectory takes the simple form

$$\omega_0\left(\mathbf{k}_a,\mathbf{q},\lambda\right) \simeq -\frac{\bar{\alpha}_s}{2}\left(\ln\frac{\mathbf{k}_a^2}{\lambda^2}+\ln\frac{\left(\mathbf{k}_a-\mathbf{q}\right)^2}{\lambda^2}\right). \tag{11}$$

With these conventions we proceed in the next section to iterate Eq. (6) to find the solution for the non–forward four–point gluon Green's function.

3 Solution to the Equation

The non–forward LL BFKL Green's function is the solution to the integral equation

$$\begin{aligned}f_\omega\left(\mathbf{k}_a,\mathbf{k}_b,\mathbf{q}\right) &= \frac{1}{\omega-\omega_0\left(\mathbf{k}_a,\mathbf{q},\lambda\right)}\left\{\delta^{(2)}\left(\mathbf{k}_a-\mathbf{k}_b\right)\right. \\ &\left.+\int\frac{d^2\mathbf{k}}{\pi\mathbf{k}^2}\theta\left(\mathbf{k}^2-\lambda^2\right)\xi\left(\mathbf{k}_a,\mathbf{k},\mathbf{q}\right)f_\omega\left(\mathbf{k}+\mathbf{k}_a,\mathbf{k}_b,\mathbf{q}\right)\right\}.\end{aligned} \tag{12}$$

for $\lambda \to 0$. If this expression is iterated, the Green's function can be expressed in terms of a kernel per iteration acting on the initial condition with a series of poles in the ω complex plane:

$$\begin{aligned} f_\omega\left(\mathbf{k}_a,\mathbf{k}_b,\mathbf{q}\right) &= \frac{\delta^{(2)}\left(\mathbf{k}_a-\mathbf{k}_b\right)}{\omega-\omega_0\left(\mathbf{k}_a,\mathbf{q},\lambda\right)} \\ &+\int\frac{d^2\mathbf{k}_1}{\pi\mathbf{k}_1^2}\frac{\theta\left(\mathbf{k}_1^2-\lambda^2\right)\,\xi\left(\mathbf{k}_a,\mathbf{k}_1,\mathbf{q}\right)}{\omega-\omega_0\left(\mathbf{k}_a,\mathbf{q},\lambda\right)}\frac{\delta^{(2)}\left(\mathbf{k}_a+\mathbf{k}_1-\mathbf{k}_b\right)}{\omega-\omega_0\left(\mathbf{k}_a+\mathbf{k}_1,\mathbf{q},\lambda\right)} \\ &+\int\frac{d^2\mathbf{k}_1}{\pi\mathbf{k}_1^2}\int\frac{d^2\mathbf{k}_2}{\pi\mathbf{k}_2^2}\frac{\theta\left(\mathbf{k}_1^2-\lambda^2\right)\,\xi\left(\mathbf{k}_a,\mathbf{k}_1,\mathbf{q}\right)}{\omega-\omega_0\left(\mathbf{k}_a,\mathbf{q},\lambda\right)}\frac{\theta\left(\mathbf{k}_2^2-\lambda^2\right)\,\xi\left(\mathbf{k}_a+\mathbf{k}_1,\mathbf{k}_2,\mathbf{q}\right)}{\omega-\omega_0\left(\mathbf{k}_a+\mathbf{k}_1,\mathbf{q},\lambda\right)} \\ &\quad\times\frac{\delta^{(2)}\left(\mathbf{k}_a+\mathbf{k}_1+\mathbf{k}_2-\mathbf{k}_b\right)}{\omega-\omega_0\left(\mathbf{k}_a+\mathbf{k}_1+\mathbf{k}_2,\mathbf{q},\lambda\right)} \\ &+\cdots \end{aligned} \tag{13}$$

Each action of the kernel corresponds to an interaction between the reggeised gluons exchanged in the t–channel, building up, in this way, the LL BFKL ladder. The poles are integrated over when going from the ω–plane to rapidity space using the Mellin transform

$$f\left(\mathbf{k}_a,\mathbf{k}_b,\mathbf{q},\mathrm{Y}\right) = \frac{1}{2\pi i}\int_{a-i\infty}^{a+i\infty}d\omega\;e^{\omega \mathrm{Y}}f_\omega\left(\mathbf{k}_a,\mathbf{k}_b,\mathbf{q}\right), \tag{14}$$

where Y is the rapidity span of the BFKL ladder.

This integration can be performed to finally obtain the solution of the non–forward LL BFKL equation for the four–point Green's function as (with $y_0 \equiv \mathrm{Y}$)

$$\begin{aligned} f(\mathbf{k}_a,\mathbf{k}_b,\mathbf{q},\mathrm{Y}) &= \left(\frac{\lambda^2}{\mathbf{k}_a^2}\frac{\lambda^2}{\left(\mathbf{k}_a-\mathbf{q}\right)^2}\right)^{\frac{\bar{\alpha}_s}{2}\mathrm{Y}}\Bigg\{\,\delta^{(2)}(\mathbf{k}_a-\mathbf{k}_b) \\ &+\sum_{n=1}^{\infty}\prod_{i=1}^{n}\int d^2\mathbf{k}_i\frac{\theta\left(\mathbf{k}_i^2-\lambda^2\right)}{\pi\mathbf{k}_i^2}\,\xi\left(\mathbf{k}_a+\sum_{l=1}^{i-1}\mathbf{k}_l,\mathbf{k}_i,\mathbf{q}\right) \\ &\times\int_0^{y_{i-1}}dy_i\left(\frac{\left(\mathbf{k}_a+\sum_{l=1}^{i-1}\mathbf{k}_l\right)^2}{\left(\mathbf{k}_a+\sum_{l=1}^{i}\mathbf{k}_l\right)^2}\frac{\left(\mathbf{k}_a+\sum_{l=1}^{i-1}\mathbf{k}_l-\mathbf{q}\right)^2}{\left(\mathbf{k}_a+\sum_{l=1}^{i}\mathbf{k}_l-\mathbf{q}\right)^2}\right)^{\frac{\bar{\alpha}_s}{2}y_i}\delta^{(2)}\left(\sum_{l=1}^{n}\mathbf{k}_l+\mathbf{k}_a-\mathbf{k}_b\right)\Bigg\}. \end{aligned} \tag{15}$$

This solution has the correct forward limit of Ref. [8] when the momentum transfer tends to zero. We would like to stress again that this method of solution is directly applicable to the non–forward BFKL equation also at NLL accuracy, with the difference that the introduction of the phase space slice is more conveniently performed in the language of dimensional regularisation.

4 Analysis of the Gluon Green's Function

To study the dependence of the non–forward LL BFKL four–point gluon Green's function on the transverse momentum scales we choose to integrate over all external angles and define the

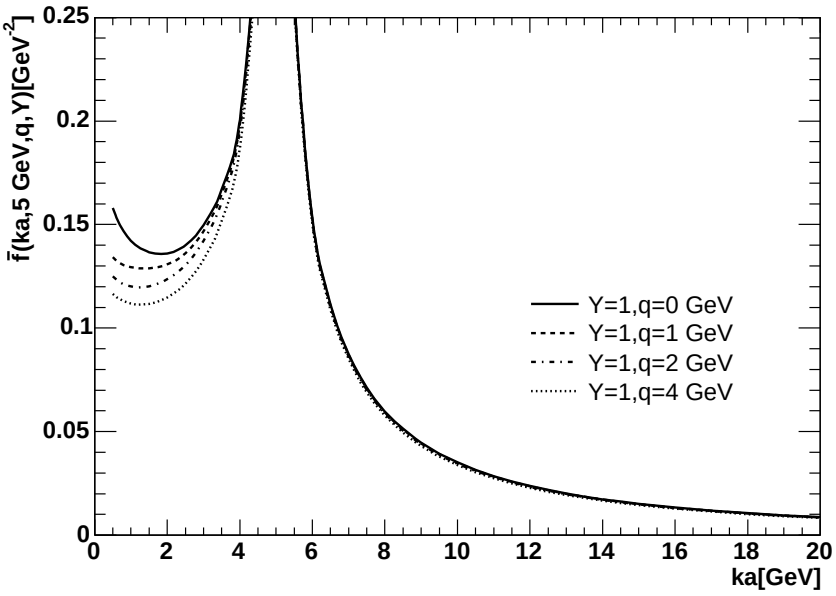

Figure 2: The angular integrated Green's function for fixed $|\mathbf{k}_b| = 5$ GeV as a function of $|\mathbf{k}_a|$ for different values of the momentum transfer. The rapidity span is low, Y = 1.

quantity

$$\bar{f}\left(|\mathbf{k}_a|, |\mathbf{k}_b|, |\mathbf{q}|, \mathrm{Y}\right) \;=\; \int_0^{2\pi} d\theta_{qa} \int_0^{2\pi} d\theta_{qb}\, f\left(\mathbf{k}_a, \mathbf{k}_b, \mathbf{q}, \mathrm{Y}\right), \tag{16}$$

where θ_{qi} is the angle between the vectors $\mathbf{k}_i$ and $\mathbf{q}$.

As a first analysis, in Fig. 2 the value of $|\mathbf{k}_b|$ is fixed to 5 GeV and the dependence on $|\mathbf{k}_a|$ is studied. When the value of the modulus of both momenta coincides, the angular integrated Green's function shows a δ–functional behaviour corresponding to the two gluon exchange limit. This dependence is caused by the driving term of the integral equation whose influence is stronger for lower energies. When Y is increased from 1 in Fig. 2 to Y = 3 in Fig. 3 the influence of the driving term diminishes as a consequence of a larger number of effective rungs in the BFKL ladder. It is interesting to note that the influence of the momentum transfer q is larger in regions of low scales of k_a. The general trend is that the four–gluon Green's function decreases with increasing q. Comparing Fig. 2 with Fig. 3 it can be seen that this effect is increasing with rapidity.

Let us now proceed to the study of the diffusion of the transverse scales in the BFKL ladder with increasing rapidity span. We choose in this analysis to concentrate on the evolution of the transverse scale along the left hand side of the ladder depicted on Fig. 1, but, as previously mentioned, one of the benefits of having the solution to the non–forward BFKL equation expressed in terms of explicit phase space integrals as in Eq. (15) is that it is possible to study any of the momenta in the ladder.

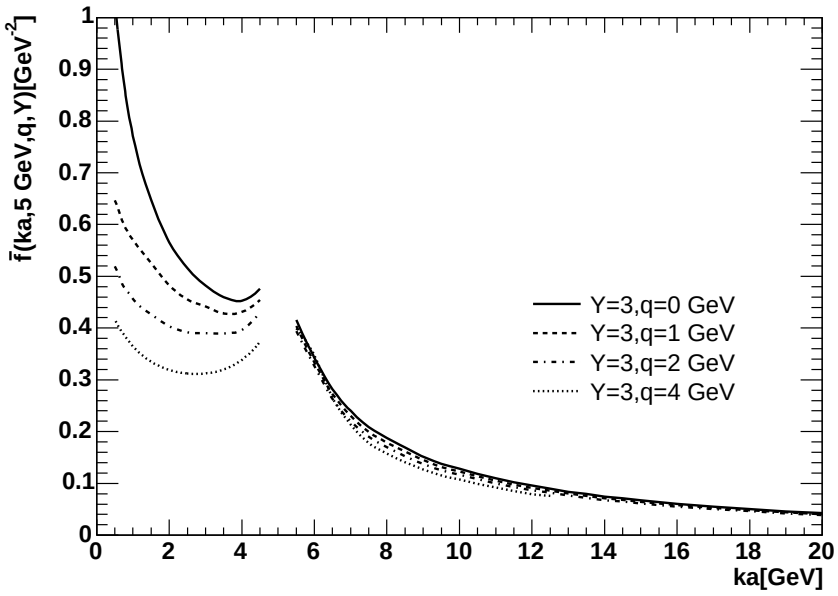

Figure 3: The angular integrated Green's function for fixed $|\mathbf{k}_b| = 5$ GeV as a function of $|\mathbf{k}_a|$ for different values of the momentum transfer q. The rapidity span is Y = 3.

Diffusion is normally studied in terms of the mean of the transverse momentum along the ladder, with the width of the distribution indicated by the standard deviation (see e.g. Ref. [13, 14]). This choice is useful, since it allows analytic studies. However, a plot of the mean internal transverse momentum plus/minus the standard deviation as a function of the rapidity along the BFKL ladder fails, by construction, to display the different behaviour of diffusion to low and high scales. Given the possibilities offered by the solution written in terms of explicit phase space integrals, we therefore choose to study diffusion in terms of the average value $\langle\tau\rangle$ of $\tau = \ln((k_a + \sum k_i)^2/\mathrm{GeV}^2)$ as a function of the rapidity Y$'$ along the ladder. Specifically, for a given value of k_a, k_b, and Y we solve the non–forward BFKL equation according to Eq. (15) by a MonteCarlo integration method. For each configuration point in $n-$momenta phase space $\{k_i, y_i\}$ we can trace the evolution of τ along the ladder and, at the same time, calculate the weight of this configuration to the total solution. In this way it is possible to calculate both the

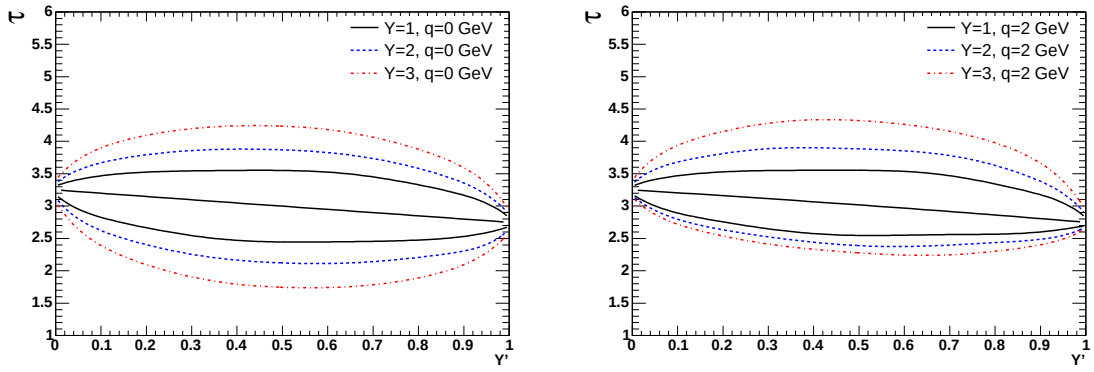

Figure 4: The diffusion properties of the gluon Green's function in terms of the lines formed by $\langle\tau\rangle$, $\langle\tau\rangle + \sigma_1$, and $\langle\tau\rangle - \sigma_2$ along the BFKL ladder. Shown for $k_a = 5$ GeV, $k_b = 4$ GeV, $q = 0$ GeV (left) and $q = 2$ GeV (right), for rapidity spans of $\mathrm{Y} = 1, 2, 3$.

average value of τ along the ladder, $\langle\tau\rangle_{(\mathrm{Y}')}$, and the quantities

$$\sigma_1^2(\mathrm{Y}') = \frac{2\displaystyle\int_{<\tau>(\mathrm{Y}')}^{\infty} d\tau(\tau - \langle\tau\rangle_{(\mathrm{Y}')})^2 \bar{f}(k_a, k_b, q, \mathrm{Y})}{\displaystyle\int_0^{\infty} d\tau \bar{f}(k_a, k_b, q, \mathrm{Y})},$$
$$\sigma_2^2(\mathrm{Y}') = \frac{2\displaystyle\int_0^{<\tau>(\mathrm{Y}')} d\tau(\tau - \langle\tau\rangle_{(\mathrm{Y}')})^2 \bar{f}(k_a, k_b, q, \mathrm{Y})}{\displaystyle\int_0^{\infty} d\tau \bar{f}(k_a, k_b, q, \mathrm{Y})}. \tag{17}$$

For a gluon Green's function $f(\mathbf{k}_a, \mathbf{k}_b, \mathbf{q}, \mathrm{Y})$ that is symmetric in τ, the lines of $\langle\tau\rangle_{(\mathrm{Y}')}$, $\langle\tau\rangle_{(\mathrm{Y}')} + \sigma_{1(\mathrm{Y}')}$, and $\langle\tau\rangle_{(\mathrm{Y}')} - \sigma_{2(\mathrm{Y}')}$ would reproduce the plot of the mean plus/minus the standard deviation. This is true for $q = 0$ GeV, as shown in Fig. 4. Here we have plotted the above mentioned three lines for $k_a = 5$ GeV, $k_b = 4$ GeV, $q = 0$ GeV, $\alpha_s = 0.23$, and $\mathrm{Y} = 1, 2, 3$. Y' is rescaled to lie between 0 and 1, so as to plot all the three cases on the same figure.

However, for $q > 0$ GeV the distribution of τ is no longer symmetric, as can be seen on the right hand side plot in Fig. 4, where we have plotted the same quantities for $q = 2$ GeV. It is apparent that there is less diffusion to smaller scales, the average is unchanged, and the diffusion to scales larger than the average is almost unchanged compared to the case $q = 0$ GeV.

It is also apparent that for the set of parameters investigated here, there is no significant diffusion into regions where the coupling is expected to become unperturbatively large. As it is well known, the influence of softer scales is larger at higher energies, but in this work we confirm the fact that the diffusion into the infrared is drastically reduced when there is some momentum transfer, acting, in this way, as an efficient infrared cut–off. It will be interesting to investigate if this picture holds at NLL.

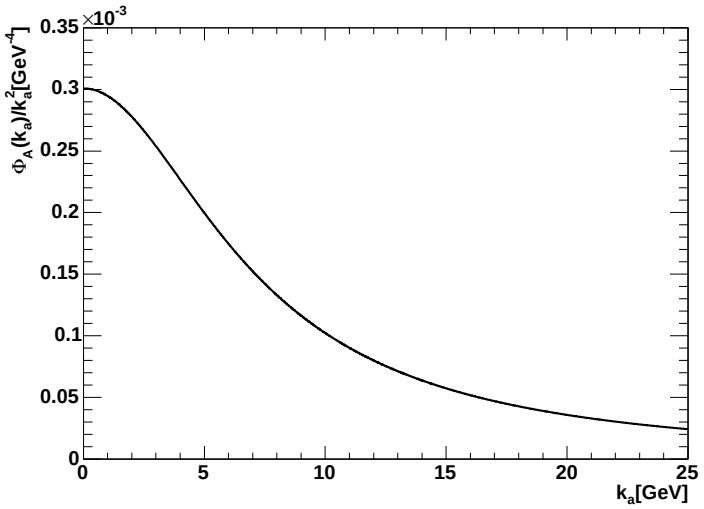

Figure 5: The impact factor $\Phi_A(k_a)/k_a^2$ for $q = 0$ GeV and $m = 3.1$ GeV.

5 Analysis of a Toy Cross–Section

Let us now turn to the study of diffractive cross–sections. To this end we need to define some suitable impact factors. We choose a generic example from Ref. [13] modelling the photo–production of a vector meson:

$$\Phi_{\rm A}(\mathbf{k}_a, \mathbf{q}) = \alpha_s h^2 \int {\rm d}\rho\, {\rm d}\tau \rho\,(1-\rho) \left[\frac{1}{(\mathbf{q}^2\rho^2\tau(1-\tau)+m^2)} - \frac{1}{((\mathbf{k}_a-\rho\,\mathbf{q})^2\tau(1-\tau)+m^2)} \right], \quad (18)$$

and similarly for $\Phi_{\rm B}$. Here, h is a normalisation constant which we choose arbitrarily such that $\alpha_s h^2 = 1$. This choice obviously means that the normalisation of the toy cross–section reported in this paper is completely arbitrary. We have plotted this impact factor divided by k_a^2 in Fig. 5 for $q = 0$ GeV and the mass of the meson $m = 3.1$ GeV. One further complication arises compared to studies of the four–point gluon Green's function due to the integration over k_a and k_b when calculating the differential cross–section as in Eq. (1). The approximations of Eqs. (5) and (11) are valid only when $\lambda \ll k_a$. When k_a is integrated over it is therefore not possible to have λ fixed. This situation is similar to the one encountered in Ref. [15]. This problem can be solved in several different ways. In the present analysis we choose to always have $\lambda < 20\,k_a$ and $\lambda \leq 1$ GeV. We have checked that the results here presented do not depend on these choices.

On Fig. 6 we have plotted the resulting cross–section of Eq. (1) as a function of the rapidity span of the BFKL ladder for $q = 0, 1, 2$ GeV, $\alpha_s = 0.2$ and $m = 3.1$ GeV. The exponential rise of the cross–section as a function of rapidity is evident for all q. In the previous section we showed how the Green's function diminishes as the momentum transfer rises, this translates here into smaller cross–sections.

In Fig. 7 we have plotted the $q-$dependence of the cross–section for rapidity spans of $Y = 0, 1, 2, 5$. We see an exponential fall–off with q for all Y. Furthermore, we observe that ${\rm d}\sigma/{\rm d}t$

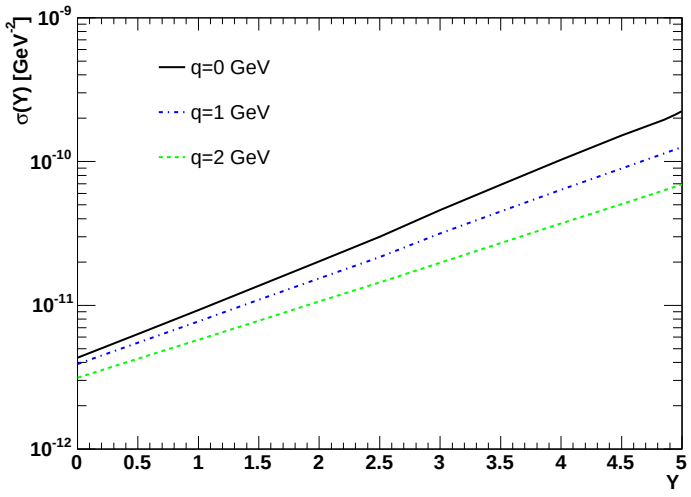

Figure 6: The toy cross–section as a function of the rapidity separation of the produced vector mesons ($m = 3.1$ GeV), each produced with transverse momentum $q = 0, 1, 2$ GeV.

at $t = 0$ GeV^2 increases with Y. The curves in Fig. 7 are presented on a linear (right) and a logarithmic (left) scale.

These results could have also been obtained using an analytic approach to solving the non–forward BFKL equation at LL accuracy. Nevertheless it is when discussing diffusion properties that the method presented in this paper has advantages. For the analysis of diffusion in cross–sections, a second issue arises compared to the study of diffusion of the Green's function. The perturbative scale is now set by both the meson mass m and the momentum transfer squared $-t$, while the scales k_a and k_b are no longer fixed. It therefore becomes interesting to study not only the distribution of the average transverse scale $\langle\tau\rangle$ along the ladder, but also at the ends of it, where it will describe the average scale of the transverse momentum connecting the impact factors to the gluon Green's function.

In Fig. 8 we have plotted the distribution of the average momentum scale in a similar way to the one used in Fig. 4 for the Green's function. It is interesting first to note that the spread along the chain is not significantly larger than that at the ends of the chain (for the rapidity spans considered here). Secondly, it is comforting to see that the typical scales remain perturbative for all values of the momentum transfer q, for the chosen value of the mass of the vector meson ($m = 3.1$ GeV). The average value of τ for $q = 0$ GeV ($\langle\tau\rangle \approx 3.9$) corresponds to a scale of the internal momenta of the BFKL exchange of roughly 7 GeV. The logarithmic scale of momenta on Fig. 4 and Fig. 8 emphasises the region of soft momenta. It might therefore be helpful to study the effect of the increase in scattering momenta on the internal scales directly: an increase of q from 0 GeV to 2 GeV leads to and increase in the upper (UV) lines corresponding to an increase in the internal momenta of roughly 2.4 GeV, while the increase in the lower (IR) lines corresponds to an increase of roughly 1.7 GeV.

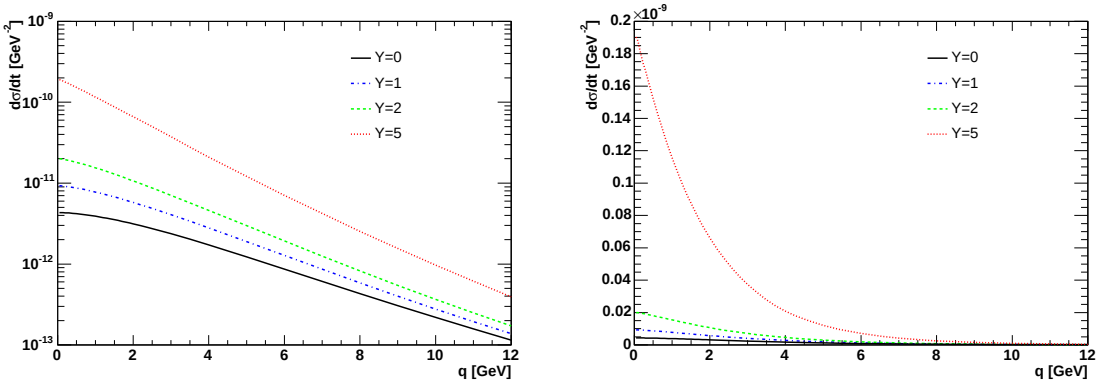

Figure 7: The toy cross–section as a function of the transverse momentum of the produced vector mesons, for rapidity separations of $\mathrm{Y} = 0, 1, 2, 5$ units of rapidity.

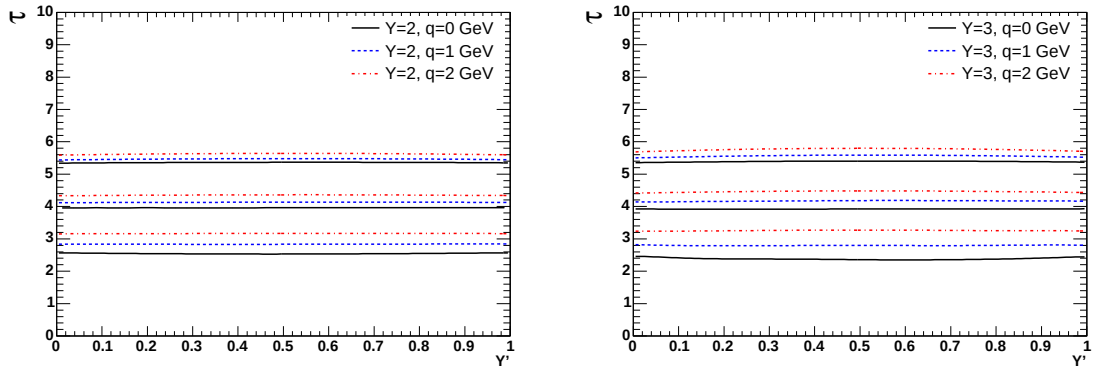

Figure 8: The range of relevant internal transverse momentum scales in terms of $\langle\tau\rangle, \langle\tau\rangle + \sigma_1, \langle\tau\rangle - \sigma_2$ for the diffractive cross– section for $\alpha_s = 0.2$, $m = 3.1$ GeV, $\mathrm{Y} = 2, 3$, and $q = 0, 1, 2$ GeV. Y' is the rescaled (to unity) rapidity along the BFKL ladder.

6 Conclusions

We have presented a new solution to the non–forward BFKL equation at leading logarithmic accuracy that allows a study of diffusion properties directly in momentum space. We have investigated the behaviour of the gluon Green's function as a function of transverse scales, including a study of the IR/UV diffusion. Then we extended this study to the analysis of a toy cross–section.

The presented framework is very efficient for solving BFKL evolution equations and the solution allows immediate insight into the momentum configurations of the evolution. We hope to extend the iterative method for solving the non–forward BFKL equation to next–to–leading logarithmic accuracy, once the appropriate integral kernel is calculated.

Acknowledgements

We acknowledge useful discussions with Jochen Bartels, Victor Fadin, Jeff Forshaw, Lev Lipatov and Leszek Motyka. ASV would like to thank the Cavendish Laboratory at the University of Cambridge and both authors wish to thank the CERN Theory Division for hospitality. JRA acknowledges the support of PPARC (postdoctoral fellowship PPA/P/S/2003/00281).

References

[1] L. N. Lipatov, Sov. J. Nucl. Phys. **23** (1976) 338 [Yad. Fiz. **23** (1976) 642],
V. S. Fadin, E. A. Kuraev and L. N. Lipatov, Phys. Lett. B **60** (1975) 50,
E. A. Kuraev, L. N. Lipatov and V. S. Fadin, Sov. Phys. JETP **44** (1976) 443 [Zh. Eksp. Teor. Fiz. **71** (1976) 840],
E. A. Kuraev, L. N. Lipatov and V. S. Fadin, Sov. Phys. JETP **45** (1977) 199 [Zh. Eksp. Teor. Fiz. **72** (1977) 377]. I. I. Balitsky and L. N. Lipatov, Sov. J. Nucl. Phys. **28** (1978) 822 [Yad. Fiz. **28** (1978) 1597],
I. I. Balitsky and L. N. Lipatov, JETP Lett. **30** (1979) 355 [Pisma Zh. Eksp. Teor. Fiz. **30** (1979) 383].

[2] S. Chekanov *et al.* [ZEUS Collaboration], Eur. Phys. J. C **26** (2003) 389,
A. Aktas *et al.* [H1 Collaboration], Phys. Lett. B **568**, 205 (2003).

[3] J. R. Forshaw and M. G. Ryskin, Z. Phys. C **68**, 137 (1995),
J. Bartels, J. R. Forshaw, H. Lotter and M. Wusthoff, Phys. Lett. B **375**, 301 (1996),
D. Y. Ivanov, Phys. Rev. D **53**, 3564 (1996),
I. F. Ginzburg and D. Y. Ivanov, Phys. Rev. D **54**, 5523 (1996),
D. Y. Ivanov and R. Kirschner, Phys. Rev. D **58**, 114026 (1998), Eur. Phys. J. C **29**, 353 (2003), Eur. Phys. J. C **36**, 43 (2004),
D. Y. Ivanov, R. Kirschner, A. Schafer and L. Szymanowski, Phys. Lett. B **478**, 101 (2000) [Erratum-ibid. B **498**, 295 (2001)],
P. Hoyer, J. T. Lenaghan, K. Tuominen and C. Vogt, Phys. Rev. D **70**, 014001 (2004),
R. Enberg, L. Motyka and G. Poludniowski, Eur. Phys. J. C **26**, 219 (2002),
J. R. Forshaw and G. Poludniowski, Eur. Phys. J. C **26**, 411 (2003),

R. Enberg, J. R. Forshaw, L. Motyka and G. Poludniowski, JHEP **0309**, 008 (2003), JHEP **0312**, 002 (2003).

[4] D. Y. Ivanov and M. Wusthoff, Eur. Phys. J. C **8** (1999) 107,
N. G. Evanson and J. R. Forshaw, Phys. Rev. D **60**, 034016 (1999).

[5] J. D. Bjorken, S. J. Brodsky and H. J. Lu, Phys. Lett. B **286**, 153 (1992),
A. H. Mueller and W. K. Tang, Phys. Lett. B **284**, 123 (1992),
M. Derrick *et al.* [ZEUS Collaboration], Phys. Lett. B **369**, 55 (1996),
F. Abe *et al.* [CDF Collaboration], Phys. Rev. Lett. **74**, 855 (1995), Phys. Rev. Lett. **80**, 1156 (1998), Phys. Rev. Lett. **81**, 5278 (1998),
B. Abbott *et al.* [D0 Collaboration], Phys. Rev. Lett. **84**, 5722 (2000),
B. Cox, J. Forshaw and L. Lonnblad, JHEP **9910**, 023 (1999),
R. Enberg, G. Ingelman and L. Motyka, Phys. Lett. B **524**, 273 (2002).

[6] L. N. Lipatov, Sov. Phys. JETP **63** (1986) 904 [Zh. Eksp. Teor. Fiz. **90** (1986) 1536].

[7] V. S. Fadin and L. N. Lipatov, Phys. Lett. B **429** (1998) 127,
M. Ciafaloni and G. Camici, Phys. Lett. B **430** (1998) 349,
D. A. Ross, Phys. Lett. B **431** (1998) 161,
G.P. Salam, JHEP**8907** (1998) 19,
C. R. Schmidt, Phys. Rev. D **60** (1999) 074003,
J. R. Forshaw, D. A. Ross and A. Sabio Vera, Phys. Lett. B **455** (1999) 273, Phys. Lett. B **498** (2001) 149,
M. Ciafaloni and D. Colferai, Phys. Lett.**B452** (1999) 372,
M. Ciafaloni, D. Colferai and G.P. Salam, Phys. Rev. **D60** (1999) 114036,
R.S. Thorne, Phys. Rev. **D60** (1999) 054031,
G. Altarelli, R. D. Ball and S. Forte, Nucl. Phys. B **575** (2000) 313, Nucl. Phys. B **621** (2002) 359, Nucl. Phys. B **674** (2003) 459,
M. Ciafaloni, D. Colferai, G. P. Salam and A. M. Stasto, Phys. Lett. B **541** (2002) 314, Phys. Rev. D **66** (2002) 054014, Phys. Lett. B **576** (2003) 143, Phys. Rev. D **68** (2003) 114003, Phys. Lett. B **587** (2004) 87.

[8] J. Kwiecinski, C. A. M. Lewis and A. D. Martin, Phys. Rev. D **54**, 6664 (1996),
C. R. Schmidt, Phys. Rev. Lett. **78**, 4531 (1997), L. H. Orr and W. J. Stirling, Phys. Rev. D **56**, 5875 (1997).

[9] J. R. Andersen and A. Sabio Vera, Phys. Lett. B **567**, 116 (2003), Nucl. Phys. B **679**, 345 (2004).

[10] J. R. Andersen and A. Sabio Vera, Nucl. Phys. B **699** (2004) 90.

[11] A. Sabio Vera, hep-ph/0307046, hep-ph/0408008,
M. Dobbs *et al.*, hep-ph/0403100,
J. R. Andersen, hep-ph/0406241.

[12] V. S. Fadin and D. A. Gorbachev, Phys. Atom. Nucl. **63**, 2157 (2000) [Yad. Fiz. **63**, 2253 (2000)], JETP Lett. **71**, 222 (2000) [Pisma Zh. Eksp. Teor. Fiz. **71**, 322 (2000)], V. S. Fadin, Nucl. Phys. Proc. Suppl. **99A**, 204 (2001).

[13] J. R. Forshaw and D. A. Ross, "Quantum chromodynamics and the pomeron", ISBN 0521 568803. Published by Cambridge University Press in the Lecture Note Series.

[14] J. Bartels, H. Lotter and M. Vogt, Phys. Lett. B **373** (1996) 215, J. Bartels and H. Lotter, Phys. Lett. B **309** (1993) 400.

[15] J. R. Andersen, V. Del Duca, S. Frixione, F. Maltoni and W. J. Stirling, hep-ph/0408239.